

Published in final edited form as:

Biomaterials. 2014 January ; 35(1): . doi:10.1016/j.biomaterials.2013.09.053.

Multifunctional silk-heparin biomaterials for vascular tissue engineering applications

F. Philipp Seib^{1,#}, Manuela Herklotz², Kelly A. Burke¹, Manfred F. Maitz², Carsten Werner^{2,3,*}, and David L. Kaplan^{1,4,*}

¹Tufts University, Department of Biomedical Engineering, 4 Colby Street Medford, MA 02155, USA

²Leibniz Institute of Polymer Research Dresden, Max Bergmann Centre for Biomaterials Dresden, Hohe Str. 6, Dresden 01069, Germany

³Center for Regenerative Therapies, Dresden University of Technology, Fetscherstraße 105, Dresden 01307, Germany

⁴Department of Chemical and Biological Engineering, 4 Colby Street Medford, MA 02155, USA

Abstract

Over the past 30 years, silk has been proposed for numerous biomedical applications that go beyond its traditional use as a suture material. Silk sutures are well tolerated in humans, but the use of silk for vascular engineering applications still requires extensive biocompatibility testing. Some studies have indicated a need to modify silk to yield a hemocompatible surface. This study examined the potential of low molecular weight heparin as a material for refining silk properties by acting as a carrier for vascular endothelial growth factor (VEGF) and improving silk hemocompatibility. Heparinized silk showed a controlled VEGF release over 6 days; the released VEGF was bioactive and supported the growth of human endothelial cells. Silk samples were then assessed using a humanized hemocompatibility system that employs whole blood and endothelial cells. The overall thrombogenic response for silk was very low and similar to the clinical reference material polytetrafluoroethylene. Despite an initial inflammatory response to silk, apparent as complement and leukocyte activation, the endothelium was maintained in a resting, anticoagulant state. The low thrombogenic response and the ability to control VEGF release support the further development of silk for vascular applications.

INTRODUCTION

Current vascular engineering approaches heavily rely on synthetic substrates such as polytetrafluoroethylene (PTFE) or polyesters that serve as a prostheses [1]. These constructs are designed to minimize intimal hyperplasia and to lower thrombogenic and inflammatory responses to retain overall function. However, the best hemocompatibility is obtained with

© 2013 Elsevier Ltd. All rights reserved.

*Corresponding authors: David L. Kaplan; Tel: +1 617-627-3251; Fax: +1 617-627-3231; David.Kaplan@tufts.edu; Carsten Werner; Tel.: +49 351 4658 532; Fax: +49-351 4658 533; werner@ipfdd.de.

#Current address: Strathclyde Institute of Pharmacy and Biomedical Sciences, University of Strathclyde, 161 Cathedral Street Glasgow G4 0RE, UK

Publisher's Disclaimer: This is a PDF file of an unedited manuscript that has been accepted for publication. As a service to our customers we are providing this early version of the manuscript. The manuscript will undergo copyediting, typesetting, and review of the resulting proof before it is published in its final citable form. Please note that during the production process errors may be discovered which could affect the content, and all legal disclaimers that apply to the journal pertain.

Disclosure statement: The authors have no competing financial interests

healthy endothelial cells, which outperform any man-made surfaces. Consequently, emerging tissue-engineering strategies either seed vascular grafts *in vitro* with endothelial cells or seek to recruit these cells *in situ* following *in vivo* implantation [2-4].

Endothelial cells are key regulators of the coagulation process; their primary physiological function is to facilitate blood flow by providing a suitable hemocompatible surface. Healthy endothelial cells are unmatched by any man-made material with respect to their hemocompatibility due to the appropriate hydrophilicity of the surface and, more importantly, due to the presence of a number of factors; for example, heparan sulfate, thrombomodulin, tissue factor pathway inhibitor, plasminogen activator, and nitrogen oxide [2, 4].

Scaffold materials with suitable biological and mechanical properties are necessary for vascular tissue engineering. One potential scaffold material of interest is silk, due to its established sericulture, aqueous processing, and its potential for fabrication into different formats such as fibers, films, gels, particles and sponges. These features are now moving the development of silk protein from a suture material to a building block for many biomedical applications including tissue engineering and drug delivery [5, 6]. Many *in vitro* studies have proposed the use of silk for vascular applications; for example, as a stent coating for sustained drug release [7], in blood vessel engineering [8], and as a material for small vascular grafts [9]. However, only a small number of studies have tested *in vivo* vascular applications of silk [9-11]. Faster and more reliable endothelialization of silk-based vascular scaffolds would further improve hemocompatibility and accelerate clinical translation.

Because no biomaterial can match the hemocompatibility of the native endothelium, strategies to improve this compatibility while exploiting suitable biomaterials (e.g., based on mechanics, remodeling rates, cell interactions) are the most viable strategies today (e.g., they avoid the need for autologous grafts with associated second site morbidity). Vascular endothelial growth factor (VEGF) is often incorporated into the design of a graft to support endothelialization *in vivo* or *ex vivo* [12]. Controlled VEGF delivery has been achieved, for example, by encapsulating this growth factor into particles (e.g., [13]) that are embedded in the scaffold [14] or by direct inclusion of VEGF into the scaffold [15]. Emerging concepts exploit the heparin binding motif of VEGF [3, 16]; heparin functionalized grafts improve VEGF release kinetics and stability in addition to modulating receptor affinity [17, 18]. ENREF 4 The bifunctional role of heparin, which serves both as a reservoir for VEGF and a means to improve hemocompatibility, makes this biopolymer particularly attractive for vascular engineering applications.

To date, a number of studies have evaluated the hemocompatibility of silk [19-21], silk alloys composed of silk and collagen [22, 23], silk and keratin [24], silk and chitosan [25], silk blends with either heparin [22] or ferulic acid [26], or silk modified chemically through sulfation [27, 28] or grafting with S-carboxymethyl keratin [24] or heparin [25]. We previously determined the impact of processing parameters on the hemocompatibility of pure silk films by using human whole blood and reference materials [29]. These studies provided an assessment of silk-associated coagulation and inflammation [29]. This type of testing is important for vascular applications because endothelial cells have the ability to respond to hemostatic and inflammatory cues in the blood stream by up-regulation of pro-coagulant proteins like tissue factor or von Willebrand factor [2, 30]. For example, silk-induced inflammation could trigger endothelial cells to switch from an antithrombotic to a prothrombotic surface. However, no studies have yet combined endothelial cells with whole blood to determine the hemocompatibility of silk.

Our aim in the present study was therefore to refine silk substrates by either covalently coupling heparin to silk or blending heparin with silk. These samples were subsequently tested for their hemocompatibility in the presence and absence of endothelial cells using human whole blood. Incubation conditions were carefully chosen to minimize blood sedimentation or the formation of a blood-air interface that could confound measurements. A silk sample selection was tested for its ability to bind and deliver heparin and/or vascular endothelial growth factor and the biological response of these factors was subsequently tested *in vitro* on human endothelial cells. [ENREF 7](#)

MATERIALS AND METHODS

Silk preparation and casting of films

Silk fibroin was extracted from *Bombyx mori* using a 30 min degumming time, as described previously [29]. Next, 1 ml of a 2 wt% silk solution was cast on polydimethylsiloxane substrates (diameter 2.5 cm) (Dow Corning Corporation, Midland USA) and allowed to dry at room temperature. Films were subsequently water vapor annealed for 6 h at 23°C for structural stabilization by inducing physical crosslinks. For cell culture studies, silk was sterile filtered through a 0.22 μ m Durapore hydrophilic PVDF membrane (Millipore, Billerica, MA, USA); all subsequent handling steps were performed in a laminar flow hood using sterile techniques. Studies that examined the ability of silk films to deliver VEGF (recombinant human VEGF-165, Shenandoah Biotechnology Inc. Warwick, PA, USA) were conducted by adding VEGF to the silk solution prior to casting. These films had a nominal VEGF loading of 2 μ g per film. For silk heparin blends, VEGF was first allowed to bind to heparin for 1 h at room temperature and then silk was added to the samples, cast, and water annealed as detailed above. This yielded films with a nominal VEGF loading of 2 μ g and either 5U or 20U of heparin.

Heparin conjugation to silk

Covalent coupling of heparin to silk was achieved using standard carbodiimide coupling chemistry (Supplementary Fig. 1). A *B. mori* silk solution was prepared as described above. The aqueous silk solution was subsequently dialyzed against a 100 mM MES (2-(*N*-morpholino)ethanesulfonic acid), Thermo Fisher Scientific, Rockford, IL, USA) buffer containing 500 mM sodium chloride at pH 6.0 for 24 h using a dialysis membrane (Thermo Fisher Scientific) with a molecular weight cutoff (MWCO) of 3500 Da. Heparin (Leo Pharma, Neu-Isenburg, Germany; M_w 6000 Da where 12 μ g of heparin is equivalent to 1U) was diluted in MES buffer by adding 1.05 ml (127 mg) of heparin to 2 ml buffer. The carboxylic acid groups of the heparin were then activated with 77.7 mg (0.405 mmol) 1-ethyl-3-(dimethylaminopropyl)carbodiimide hydrochloride (EDC, 2.13 mol/mol COOH) and 120 mg (1.04 mmol) *N*-hydroxysuccinimide (NHS, 5.48 mol/mol COOH), both obtained from Thermo Fisher Scientific. The number of COOH groups on heparin was estimated from the literature to be 9 mol COOH/mol heparin [31]. Activation proceeded at room temperature for 15 min with magnetic stirring. After 15 min, 284 μ l (4.06 mmol) 2-mercaptoethanol (Sigma-Aldrich, St. Louis, MO, USA) was added to the reaction to quench the EDC (10 mol/mol EDC). Next, 37.1 ml of a 3.08% (w/v) silk solution (1.14 g silk) was added to the reaction and the pH was raised to 6.6 by dropwise addition of 100 mM sodium hydroxide. The reaction, which coupled the COOH of heparin to primary amine functional groups on silk fibroin, was carried out for 5.5 h under magnetic stirring at room temperature. The reaction was then quenched with an aqueous hydroxylamine solution (Sigma-Aldrich, 5 mol hydroxylamine/mol NHS) to convert unreacted NHS groups on heparin to hydroxamic acid groups. The solution was transferred to dialysis cassettes (MWCO 20,000) to remove unreacted heparin by extensive dialysis against 100 mM Na_2HPO_4 and subsequently ddH_2O for 72 h. The degree of silk fibroin functionalization with heparin was determined using

elemental analysis (carbon, hydrogen, nitrogen by combustion and sulfur by titration) at Elemental Analysis Inc. (Lexington, KY, USA). Films of pure silk, a 10% w/w blend of heparin with silk, and the heparin functionalized silk were prepared and analyzed. The weight fractions of C, H, and N in heparin were determined using the analysis of the pure silk and the known blend. These weight fractions and balances on the elements were used to calculate the weight fraction of heparin in the silk heparin conjugate. Sample films were prepared as detailed above.

Sample nomenclature

Different silk films were produced: (1) pure silk film (denoted as silk); (2) silk films containing 20U with heparin added (denoted as silk + 20U heparin blend); (3) silk film containing 5U of heparin added (denoted as silk + 5U heparin blend); (4) silk film containing 20U of covalently conjugated heparin (denoted as silk 20U heparin conjugate) that served as a control in the hemocompatibility studies (detailed below); and (5) inclusion of VEGF into selected film preparations, as detailed below (denoted as +VEGF).

Heparin and VEGF release kinetics

Heparin and VEGF release were determined by incubating samples with 1 ml of PBS at room temperature, with daily buffer changes. Assay samples were stored at -80°C and analyzed using a human VEGF (VEGF-165) DuoSet ELISA (R&D Systems Minneapolis, MN, USA) and a 1, 9-dimethylmethylene blue-based colorimetric assay (Blyscan assay, Bicolor Ltd, Carrickfergus, United Kingdom) according to the manufacturers' instructions.

Cell culture: biological response towards functionalized silk films

Human umbilical cord venous endothelial cells (HUVECs) were either isolated from fresh umbilical cords (approved by the ethics review board of Dresden University of Technology) [32] or purchased (Lonza, Walkersville MD, USA). The cells were maintained in a humidified atmosphere of 5% CO_2 at 37°C , and cultures were routinely subcultured every 3 to 6 days when a confluency of 70% was reached, unless specified otherwise. Cells were kept in culture up to passage 5. HUVECs were routinely grown in endothelial basal growth medium (EBM-2, CC-3156, Lonza Rochester, NY, USA) and supplemented with a SingleQuot bullet kit (CC-4176, Lonza) that contained fetal bovine serum (FBS), hydrocortisone, ascorbic acid, heparin, VEGF, fibroblast growth factor-basic (hFGF-B), insulin-like growth factor-I with the substitution of arginine for glutamic acid at position 3 (R3-IGF-1), human epidermal growth factor (hEGF), gentamicin, and amphotericin-B (GA-1000).

The biological response of HUVECs towards VEGF was determined by plating cells at a density of 5.0×10^3 cells/ cm^2 in complete culture medium in 6 well plates and allowing them to recover overnight. Next, cultures were washed with PBS and a minimum culture medium (EBM-2) that contained only GA-1000 and reduced FBS levels (i.e., a 50-fold reduction when compared with the parent formulation). Control silk films, films with VEGF and/or heparin, and freely diffusible VEGF or heparin at equivalent concentrations were added to the cultures in 6 well plates. After a 3 day incubation, the films were removed and the metabolic activity of the cells was determined with a 5 mg/ml substrate concentration of (3-(4,5-dimethylthiazol-2-yl)-2,5-diphenyltetrazolium bromide (MTT); for 6 well cultures, 500 μl of substrate was added to the cultures. Following a 5 h incubation period, formazan was solubilized with 1 ml of dimethylsulfoxide, and the absorbance was measured at 560 nm.

For hemocompatibility studies in the presence of HUVECs, glass coverslips (diameter 2.50 cm) were surface functionalized with poly(octadecen-*alt*-maleic anhydride) followed by the

covalent attachment of fibronectin from a 50 µg/ml solution, as detailed previously [33]. Next, HUVECs were plated in complete growth medium at a density of 1.7×10^4 cells/cm². Cultures were allowed to establish themselves for 8 days and confluent cultures were used for the blood studies detailed below.

Hemocompatibility testing of silk films

All studies were approved by the ethics board and complied with institutional and international guidelines (review board of Dresden University of Technology). Studies were performed in two independent incubations, each with a triplicate set of samples. The blood for the two incubations was pooled from different pairs of ABO matched volunteers. We ensured that donors were not taking any medication that could interfere with the blood coagulation cascade and had not taken nonsteroidal antiinflammatory drugs in the past 10 days.

The freshly drawn heparin-anticoagulated (1 IU/ml) whole blood was added to the sample chambers as detailed below [29]. Respective silk films and either a PTFE film or an endothelial monolayer were mounted on either side of a 6.4 mm thick incubation chamber [34], exposing 3.1 cm² of the respective surface (Fig. 1). To these samples, 2 ml of blood was added, taking care to avoid formation of a blood-air interface. The incubation chambers were kept at 37°C under constant overhead rotations of about six revolutions/min for 2 h. Next, blood samples were mixed with the recommended stabilizers according to the manuals of the ELISA test kits, centrifuged, and the plasma was stored at –80°C until analysis. Plasma coagulation and blood platelet activation were measured by determining the amount of prothrombin F1+2 fragment (Enzygnost F1+2 micro, Siemens, Eschborn, Germany) and platelet factor 4 (PF4) (Zymutest PF4, CoaChrom, Vienna Austria), respectively, according to the manufacturers' instructions. Complement activation was determined by measuring C5a fragment (DRG Instruments, Marburg, Germany), Bb and C4d (Quidel, San Diego, CA, USA) by ELISA. Cell surface markers for CD11b (clone ICRF44, Biozol, Eching, Germany) and CD41a (clone HIP8, Becton Dickinson, Heidelberg, Germany) were analyzed by flow cytometry (FACSCalibur, Becton Dickinson, Heidelberg, Germany) to determine leukocyte activation and granulocyte-platelet conjugates, respectively. Details of the flow cytometric analysis have been described previously [29].

Electron microscopy

Samples were fixed with phosphate buffered 2 wt% glutaraldehyde, dehydrated, critical point dried, sputter coated with gold, and imaged with a scanning electron microscope (FEI-Philips, Eindhoven Netherlands), as described previously [29].

Statistical analysis

Data were analyzed using GraphPad Instat 5.0b (GraphPad Software, La Jolla USA). Sample pairs were analyzed with the Student's *t*-test. Multiple samples were evaluated by one-way analysis of variance (ANOVA) followed by Bonferroni or Dunnett's post hoc tests to evaluate the statistical differences ($P < 0.05$) among all samples or between samples and controls, respectively. All error bars are standard deviation (SD).

RESULTS

Release characteristics of heparin and VEGF from silk blends and the subsequent biological response

Silk heparin blends were first tested for their ability to release heparin (Fig. 2). Over the first 10 h, a faster relative heparin release was seen for the 20U silk blends than for the 5U

blends, while at later time points the release profiles for both systems were comparable. During the first 60 minutes of the release study, 48% and 30% of the total heparin was released from the 20U and 5U silk heparin blends, respectively. Both preparations released >90% of their heparin loads over 6 days.

The release characteristics of VEGF loaded silk films were then tested. Significantly more rapid release was observed from silk films that only contained VEGF than from any of the heparin blends. Both heparin blends showed comparable VEGF release kinetics. At the end of the release study, approximately 3 times more VEGF had been released from the silk films than from the heparin blends. The impact of VEGF on endothelial cells was evaluated by generating a dose-response curve (Fig. 3a). A diffusible VEGF concentration >0.2 ng/ml was required to induce cell proliferation, with a notable biological response for >2 to 200 ng/ml of diffusible VEGF. Similar to these control studies, the inclusion of VEGF into silk films significantly improved endothelial viability (Fig. 3b).

Hemocompatibility of functionalized silk

Next, the blood compatibility of the silk was studied. The hemocompatibility test system was further refined by including viable endothelial cells in the setup to generate a fully humanized test system (Fig. 1). Because heparin released from the blends inevitably inhibits coagulation and might mask other pro-coagulant effects, a control was prepared where heparin was covalently conjugated to silk. The synthetic strategy employed EDC/NHS coupling chemistry to generate a silk-heparin conjugate (Supplementary Fig. 1). Use of a 28 fold molar excess of carboxylic acid functional groups on heparin relative to primary amine groups of silk resulted in functionalization of 59% of the available reactive sites, a conjugate that was 2.1% heparin by weight, and an overall reaction yield of approximately 85%. This silk-heparin conjugate was then diluted with silk and cast on PDMS, as detailed above, to generate films (20U of heparin per film) that were water annealed and subsequently tested for their ability to influence the blood coagulation cascade.

Hemostasis response

The inflammatory and hemostasis parameters induced by silk substrates were determined using human whole blood in the presence and absence of endothelial cells (Fig. 1). Pure silk samples and silk blends with 5U of heparin were co-incubated with endothelial cells, resulting in reduced coagulation determined using prothrombin F1+2 fragment as an indicator. The silk blends with 5U of heparin outperformed the clinical reference material PTFE (Fig. 4). The silk heparin conjugate and the PTFE sample showed a similar response in the presence or absence of endothelial cells (Fig. 4). However, silk heparin blends with 20U of heparin showed a substantial increase in prothrombin fragments, which was highest when samples were co-incubated with endothelial cells. The extent of platelet activation was evaluated by measuring the PF4 levels in the blood plasma (Fig. 4). Silk heparin conjugates and the corresponding silk blend with 20U of heparin showed the highest PF4 levels of any tested substrate when co-incubated with endothelial cells. However, endothelial cells reduced platelet activation in the PTFE control group and had no effect on the remaining silk samples. In the absence of endothelial cells, all silk substrates showed a response that was similar to the clinical reference material PTFE. The PF4 measurements were complemented by determining the degree of granulocyte-platelet conjugate formation. Differences between samples incubated in the presence and absence of endothelial cells were marginal, although the silk heparin conjugate and the corresponding silk blend with 20U of heparin showed elevated levels of granulocyte-platelet conjugates.

Inflammatory response to silk substrates

In parallel with the coagulation activation, the inflammatory response towards modified silk substrates was also determined (Fig. 5). The common C5a complement factor was significantly elevated for many silk samples when compared to PTFE; no differences were noted between the endothelial test system and the incubation without endothelium (Fig. 5a). Activation of the complement cascade via the classical or alternative pathway was evaluated by measuring the complement fragments Bb and C4d to serve as indicators of the alternative and classical pathway, respectively. C4d levels for all test samples were close to the initial level (Fig. 5b). In contrast, activation of the alternative pathway was evident because Bb levels were significantly increased compared to the initial blood and significantly higher levels were induced in the silk samples than in the PTFE control (Fig. 5b). The silk +20U heparin blend had one of the highest Bb levels. Co-incubation with endothelial cells significantly reduced Bb activation for pure silk and substantially for silk blend with 5U of heparin. An impact of endothelial cells on the other silk samples was not readily apparent. However, PTFE reference samples showed some improvement when endothelial cells were present. This analysis was complemented by determining the activation of leukocytes by measuring leukocyte CD11b expression (Fig. 5a). The results emulated the trends seen for C5a, as PTFE showed the lowest CD11b expression levels while significantly higher expression levels were observed for the silk heparin conjugate in the presence of endothelial cells.

Scanning electron microscopy was used to visualize the interaction of blood cells with the test substrates (Fig. 6). For example, leukocytes appeared more widespread on the silk samples than on PTFE although the extent of platelet adhesion was similar for all test samples. The studies that included endothelial monolayers revealed a similar appearance of the endothelial surface for all samples, with no apparent differences between the groups (Fig. 7). The endothelium was sparsely populated by platelets and leukocytes (Fig. 7a). The platelets showed some pseudopodia formation whereas the leukocytes showed no signs of activation (e.g., pseudopodia). Spreading granulocytes were absent from all endothelial samples (Fig. 7d).

DISCUSSION

The use of silk as a suture material dates back many centuries. While a myriad of synthetic polymers have been developed as suture materials, silk continues to show unmatched toughness, strength, and extensibility [35]. The clinical portfolio of silk-based products has recently been expanded and now also includes surgical meshes (Allergan Inc., Irvine, CA, USA). Ongoing research and development efforts now support the use of silk beyond load bearing applications; for example, in tissue engineering [5]. The ability of silk to support endothelial growth both *in vitro* and *in vivo* bodes well for the use of this material in vascular engineering applications (e.g., [9, 36, 37]). Engineering of vascular tissues requires reliable endothelialization because a healthy endothelium presents the best known hemocompatible surface. One possibility for achieving this hemocompatibility is by facilitating endothelial ingrowth into a silk graft, which would require the material to minimize thrombosis and to support endothelialization. This, in turn, means that the material must be able to maintain the endothelium in a resting, anticoagulant state.

In the present study, we functionalized silk with VEGF-165 with the view of supporting endothelialization. VEGF-165 is a 38.2 kDa protein with a near neutral isoelectric point of 7.88; it contains a heparin binding site, which requires N-sulfation and 6-O sulfation of the polysaccharide [38]. The fast release of VEGF from the unmodified silk film indicated that the cationic residues of the heparin binding site did not have a strong affinity for the anionic silk. However, integration of heparin into the silk allowed controlled heparin release for 6

days. Heparin binding of VEGF further stabilizes the growth factor, preventing it from degradation by endogenous proteases and can also enhance its receptor activity [17, 18].

Many tissue engineering applications exploit heparin to retain VEGF and control its release [6]. However, various clinical concerns are raised against the application of heparin to surfaces during vascular engineering applications. Heparin can influence platelet, monocyte, and neutrophil function *in vitro* [39]; the most important reaction is the clinical risk of life-threatening heparin induced thrombocytopenia type II [40]. These disadvantages can be addressed by the use of low molecular weight heparins instead of unfractionated heparin [39, 41]. We used the low molecular weight heparin Tinzaparin to functionalize silk; no other previous study has used this fractionated heparin in combination with silk [22, 23, 25, 42].

The affinity of low molecular weight heparin towards VEGF [43] varies and is in part product specific. Low molecular weight heparin may stimulate or suppress angiogenesis upon systemic administration, which is thought to reflect a product dependence [44-46], but no information is available for immobilized low molecular weight heparin [44, 47]. In the present study, VEGF containing silk-heparin blends significantly supported endothelial growth and maximized the biological effect. In this context, Tinzaparin showed no noticeable antiangiogenic effect. VEGF-containing silk heparin blends employing Tinzaparin appeared to be a suitable scaffold material for vascular engineering applications as they supported endothelialization without the risk of heparin induced thrombocytopenia type II. Further support for the use of heparinized silk is the observation that these constructs stimulated elastic fiber formation *in vivo* as part of the endothelialization process [48].

Next, we subjected a range of silk samples to hemocompatibility testing. We previously showed that silk induced a low thrombogenic response that was similar to the clinical reference material PTFE [29]. However, silk induced an inflammatory response that was significantly higher than observed with PTFE [29]. A healthy endothelium is known to respond to inflammatory reactions in the blood by switching from an anti- to pro-coagulant phenotype [2, 4, 30]. This knowledge motivated us to determine the hemocompatibility of silk samples in the presence of endothelial cells, to determine if silk could induce the pro-coagulant phenotype in the endothelium. Therefore, heparin not only served to control VEGF release but also improved coagulation and inflammation. Heparin is a clinically well-known indirect anticoagulant, which enhances the inhibitory effect of antithrombin. Furthermore, heparin impacts various interactions of the inflammatory complement cascade. Physiologically, polyanionic glucosaminoglycans like heparan sulfate and heparin, when present on the surface of cells, contribute to the protection against self-attack by the complement system. Specifically, the regulatory complement factor H has a high affinity for heparin. In concert with factor I, it regulates the alternative complement pathway by degrading complement C3b and the C3bBb-convertase [49]. We therefore expected that the inclusion of heparin into silk would block the complement activation and related leukocyte activation.

We examined the ability of heparin modified silk substrates to influence the inflammatory response. Significantly less inflammation was induced by the PTFE reference material than by any of the silk substrates, as judged by the total complement activation using the complement fragment C5a as an indicator (Fig. 5a). Endothelial cells could further decrease the complement concentration for PTFE samples, but the silk samples showed no marked difference when endothelial cells were included in the test system (Fig. 5a). Silk substrates appeared to activate the complement cascade in this *in vitro* system; modifying the substrates with heparin or refining the incubation studies with endothelial cells were not

sufficient strategies to modulate the response. The increased inflammatory response, however, did not induce the endothelium to switch to a pro-coagulant phenotype.

The trends observed with C5a were mirrored by the extent of leukocyte activation (CD11b) (Fig. 5a). C5a is among the strongest activators of leukocytes. The close correlation of CD11b with the C5a concentration indicated that no factors independent of complement caused leukocyte activation. These *in vitro* studies suggested that silk can induce a temporary inflammatory response, but how these measurements directly impact the *in vivo* performance of silk as a vascular graft remain to be investigated. *In vivo* studies employing silk consistently showed that silk-based grafts had a low thrombogenic response, improved vascular patency, substantial endothelial ingrowth, and a lower foreign body response when compared to PTFE [9-11]. It therefore appears that the short term *in vitro* performance does not necessarily translate directly to long term *in vivo* outcomes.

The complement system is activated through either the classical pathway (involving the complement factor C4d) or the alternative pathway (involving Bb). Only significant Bb differences between the initial value, PTFE, and the silk substrates suggested that the alternative pathway was responsible for the observed inflammatory response. The alternative pathway has evolved to tackle any foreign surface; for example, bacterial polysaccharides, fungi, and biomaterials. It is therefore the first-line defense mechanism, due to its immediate responsiveness, because this pathway does not require antibody or immune complexes [50]. In the body, protection from auto-aggression by the alternative pathway is achieved through the cell surface expression of heparin-like molecules. For the present study, heparinization of the silk substrates could not take on this role. This is in contrast to the situation seen with dialysis membranes [51] or model substrates [52], where heparin grafting reduced complement activation. However, all these studies used unfractionated heparin, which has superior factor H complexation when compared to low molecular weight heparin [53]. Therefore, the insufficient length and/or accessibility of the low molecular weight heparin used in the present study could have contributed to the unexpected results.

In a parallel set of studies, we examined the thrombogenic response. We were able to verify previous observations that silk has a low thrombogenic potential that matches the benchmark set by PTFE [29]. This benchmark was met by silk samples without modification and by heparin-releasing silk-heparin blends (Silk + 5U heparin blend); even lower coagulation was induced by the silk heparin conjugate than by PTFE (Fig. 4). The present study subjected silk substrates to more physiologically relevant hemocompatibility by exposing samples simultaneously to whole blood and human endothelium (Fig. 1). In turn, this allowed us to probe the effect of biomaterial-activated blood on endothelium.

In general, the thrombogenic response of silk substrates co-incubated with endothelial cells either reduced coagulation activation (prothrombin F1+2 fragment) or maintained it at a low level. This can be attributed to the active anticoagulant property of the endothelium surface. Inclusion of the endothelium did not have a significant impact on the overall outcome because coagulation was already very low for most samples, offering little room for further improvement. An exception was the Silk + 20U heparin blend, which was associated with significantly elevated coagulation (prothrombin F1+2 fragment), raised PF4 (Fig. 4), and elevated Bb of the alternative pathway, but no differences for the terminal pathway of the complement cascade (C5a) or leukocyte activation (CD11b). The elevated coagulation activation observed with the Silk + 20U heparin blend sample in endothelial co-incubation studies may be a result of endothelium activation. Although not determined in the present study, freely diffusible silk protein can induce blood coagulation [27], thereby contributing to a switch of the endothelium to a procoagulant state. Future studies will examine the endothelium phenotype and its response to freely diffusible silk.

This study to employ a panel of markers to determine the hemocompatibility of silk by simultaneously examining hemostasis and inflammation in the presence and absence of endothelial cells. Previous reports have applied various functional coagulation tests to analyse heparin modified silk films or fibers (e.g., [22, 23, 25, 42]). All these studies reported improvement of the clotting parameters but did not examine the inflammatory response towards silk and its potential effect on the anticoagulant state of endothelial cells. In the present study, higher inflammation was induced by the high release silk blend with 20U heparin than by the other silk samples; this was only observed during co-incubation studies with endothelial cells. This finding suggests that biomaterials can convert the endothelium from an anticoagulant to a pro-coagulant state *in vitro*, highlighting the critical role of a functional endothelium when performing hemocompatibility testing.

CONCLUSIONS

A library of heparin modified silk substrates were generated, tested for their hemocompatibility using human whole blood, and evaluated for their potential to control VEGF release. Heparinized silk can be used to generate dual-functional materials with improved hemocompatibility and controlled growth factor release. We included endothelial cells in our *in vitro* blood studies to better mimic the biomaterial-endothelial interface. This study provides proof of principle that such a test system can be successfully used to study hemocompatibility of biomaterials.

Supplementary Material

Refer to Web version on PubMed Central for supplementary material.

Acknowledgments

The authors would like to thank Monique Marx and Martina Franke, Leibniz Institute of Polymer Research Dresden for technical assistance. This work was supported by NIH grant P41 EB002520-05 (Tissue Engineering Resource Center) (DLK), KAB is supported by a Ruth Kirchstein Postdoctoral Fellowship awarded by the National Institute of Diabetes and Digestive and Kidney Diseases (Grant Number F32DK093194) and FPS was supported by a Mildred Scheel Postdoctoral fellowship from the German Cancer Aid and a Marie Curie FP7 Career Integration Grant PCIG12-GA-2012-334134 within the 7th European Union Framework Programme.

REFERENCES

- [1]. Bordenave L, Menu P, Baquey C. Developments towards tissue-engineered, small-diameter arterial substitutes. *Expert Rev Med Devices*. 2008; 5:337–47. [PubMed: 18452384]
- [2]. Achneck HE, Sileshi B, Parikh A, Milano CA, Welsby IJ, Lawson JH. Pathophysiology of bleeding and clotting in the cardiac surgery patient: from vascular endothelium to circulatory assist device surface. *Circulation*. 2010; 122:2068–77. [PubMed: 21098468]
- [3]. Liu S, Liu T, Chen J, Maitz M, Chen C, Huang N. Influence of a layer-by-layer-assembled multilayer of anti-CD34 antibody, vascular endothelial growth factor, and heparin on the endothelialization and anticoagulation of titanium surface. *J Biomed Mater Res A*. 2013; 101:1144–57. [PubMed: 23045161]
- [4]. McGuigan AP, Sefton MV. The influence of biomaterials on endothelial cell thrombogenicity. *Biomaterials*. 2007; 28:2547–71. [PubMed: 17316788]
- [5]. Kasoju N, Bora U. Silk fibroin in tissue engineering. *Adv Healthc Mater*. 2012; 1:393–412. [PubMed: 23184771]
- [6]. Wenk E, Merkle HP, Meinel L. Silk fibroin as a vehicle for drug delivery applications. *J Control Release*. 2011; 150:128–41. [PubMed: 21059377]
- [7]. Pan CJ, Shao ZY, Tang JJ, Wang J, Huang N. In vitro studies of platelet adhesion, activation, and protein adsorption on curcumin-eluting biodegradable stent materials. *J Biomed Mater Res A*. 2007; 82:740–6. [PubMed: 17326229]

- [8]. Domachuk P, Tsioris K, Omenetto FG, Kaplan DL. Bio-microfluidics: biomaterials and biomimetic designs. *Adv Mater.* 2010; 22:249–60. [PubMed: 20217686]
- [9]. Enomoto S, Sumi M, Kajimoto K, Nakazawa Y, Takahashi R, Takabayashi C, et al. Long-term patency of small-diameter vascular graft made from fibroin, a silk-based biodegradable material. *J Vasc Surg.* 2010; 51:155–64. [PubMed: 19954921]
- [10]. Christenson JT, Eklof B, Al-Huneidi W, Owunwanne A. Elastic and thrombogenic properties for different vascular grafts and its influence on graft patency. *Int Angiol.* 1987; 6:81–7. [PubMed: 3624952]
- [11]. Huang F, Sun L, Zheng J. In vitro and in vivo characterization of a silk fibroin-coated polyester vascular prosthesis. *Artif Organs.* 2008; 32:932–41. [PubMed: 19133021]
- [12]. Lovett M, Lee K, Edwards A, Kaplan DL. Vascularization strategies for tissue engineering. *Tissue Eng Part B Rev.* 2009; 15:353–70. [PubMed: 19496677]
- [13]. Peters MC, Isenberg BC, Rowley JA, Mooney DJ. Release from alginate enhances the biological activity of vascular endothelial growth factor. *J Biomater Sci Polym Ed.* 1998; 9:1267–78. [PubMed: 9860169]
- [14]. Richardson TP, Peters MC, Ennett AB, Mooney DJ. Polymeric system for dual growth factor delivery. *Nat Biotechnol.* 2001; 19:1029–34. [PubMed: 11689847]
- [15]. Kaigler D, Wang Z, Horger K, Mooney DJ, Krebsbach PH. VEGF scaffolds enhance angiogenesis and bone regeneration in irradiated osseous defects. *J Bone Miner Res.* 2006; 21:735–44. [PubMed: 16734388]
- [16]. Zieris A, Chwalek K, Prokoph S, Levental KR, Welzel PB, Freudenberg U, et al. Dual independent delivery of pro-angiogenic growth factors from starPEG-heparin hydrogels. *J Control Release.* 2011; 156:28–36. [PubMed: 21763368]
- [17]. Ashikari-Hada S, Habuchi H, Kariya Y, Kimata K. Heparin regulates vascular endothelial growth factor165-dependent mitogenic activity, tube formation, and its receptor phosphorylation of human endothelial cells. Comparison of the effects of heparin and modified heparins. *J Biol Chem.* 2005; 280:31508–15. [PubMed: 16027124]
- [18]. Nishiguchi KM, Kataoka K, Kachi S, Komeima K, Terasaki H. Regulation of pathologic retinal angiogenesis in mice and inhibition of VEGF-VEGFR2 binding by soluble heparan sulfate. *PLoS One.* 2010; 5:e13493. [PubMed: 20975989]
- [19]. Motta A, Maniglio D, Migliaresi C, Kim HJ, Wan X, Hu X, et al. Silk fibroin processing and thrombogenic responses. *J Biomater Sci Polym Ed.* 2009; 20:1875–97. [PubMed: 19793445]
- [20]. Motta A, Migliaresi C, Lloyd AW, Denyer SP, Santin M. Serum protein absorption on silk fibroin fibers and films: Surface opsonization and binding strength. *J Bioact Compat Polym.* 2002; 17:23–35.
- [21]. Santin M, Denyer SP, Lloyd AW, Motta A. Domain-driven binding of fibrin(ogen) onto silk fibroin biomaterials. *J Bioact Compat Polym.* 2002; 17:195–208.
- [22]. Lu Q, Zhang S, Hu K, Feng Q, Cao C, Cui F. Cytocompatibility and blood compatibility of multifunctional fibroin/collagen/heparin scaffolds. *Biomaterials.* 2007; 28:2306–13. [PubMed: 17292467]
- [23]. Tang Y, Cao C, Ma X, Chen C, Zhu H. Study on the preparation of collagen-modified silk fibroin films and their properties. *Biomed Mater.* 2006; 1:242–6. [PubMed: 18458412]
- [24]. Lee KY, Kong SJ, Park WH, Ha WS, Kwon IC. Effect of surface properties on the antithrombogenicity of silk fibroin/S-carboxymethyl kerateine blend films. *J Biomater Sci Polym Ed.* 1998; 9:905–14. [PubMed: 9747984]
- [25]. Wang J, Hu W, Liu Q, Zhang S. Dual-functional composite with anticoagulant and antibacterial properties based on heparinized silk fibroin and chitosan. *Colloids Surf B Biointerfaces.* 2011; 85:241–7. [PubMed: 21459560]
- [26]. Wang S, Gao Z, Chen X, Lian X, Zhu H, Zheng J, et al. The anticoagulant ability of ferulic acid and its applications for improving the blood compatibility of silk fibroin. *Biomed Mater.* 2008; 3:044106. [PubMed: 19029605]
- [27]. Tamada Y. Sulfation of silk fibroin by chlorosulfonic acid and the anticoagulant activity. *Biomaterials.* 2004; 25:377–83. [PubMed: 14585685]

- [28]. Ma X, Cao C, Zhu H. The biocompatibility of silk fibroin films containing sulfonated silk fibroin. *J Biomed Mater Res Part B Appl Biomater*. 2006; 78:89–96. [PubMed: 16292767]
- [29]. Seib FP, Maitz MF, Hu X, Werner C, Kaplan DL. Impact of processing parameters on the haemocompatibility of Bombyx mori silk films. *Biomaterials*. 2012; 33:1017–23. [PubMed: 22079005]
- [30]. Cines DB, Pollak ES, Buck CA, Loscalzo J, Zimmerman GA, McEver RP, et al. Endothelial cells in physiology and in the pathophysiology of vascular disorders. *Blood*. 1998; 91:3527–61. [PubMed: 9572988]
- [31]. Gatti G, Casu B, Hamer GK, Perlin AS. Studies on the conformation of heparin by ¹H and ¹³C NMR Spectroscopy. *Macromolecules*. 1979; 12:1001–7.
- [32]. Weis JR, Sun B, Rodgers GM. Improved method of human umbilical arterial endothelial cell culture. *Thromb Res*. 1991; 61:171–3. [PubMed: 2020944]
- [33]. Herklotz M, Werner C, Pompe T. The impact of primary and secondary ligand coupling on extracellular matrix characteristics and formation of endothelial capillaries. *Biomaterials*. 2009; 30:35–44. [PubMed: 18838154]
- [34]. Streller U, Sperling C, Hubner J, Hanke R, Werner C. Design and evaluation of novel blood incubation systems for in vitro hemocompatibility assessment of planar solid surfaces. *J Biomed Mater Res Part B Appl Biomater*. 2003; 66B:379–90. [PubMed: 12808598]
- [35]. Omenetto FG, Kaplan DL. New opportunities for an ancient material. *Science*. 2010; 329:528–31. [PubMed: 20671180]
- [36]. Cattaneo I, Figliuzzi M, Azzollini N, Catto V, Fare S, Tanzi MC, et al. In vivo regeneration of elastic lamina on fibroin biodegradable vascular scaffold. *Int J Artif Organs*. 2013; 36:166–74. [PubMed: 23404641]
- [37]. Unger RE, Peters K, Wolf M, Motta A, Migliaresi C, Kirkpatrick CJ. Endothelialization of a non-woven silk fibroin net for use in tissue engineering: growth and gene regulation of human endothelial cells. *Biomaterials*. 2004; 25:5137–46. [PubMed: 15109837]
- [38]. Ono K, Hattori H, Takeshita S, Kurita A, Ishihara M. Structural features in heparin that interact with VEGF165 and modulate its biological activity. *Glycobiology*. 1999; 9:705–11. [PubMed: 10362840]
- [39]. Engstad CS, Gutteberg TJ, Osterud B. Modulation of blood cell activation by four commonly used anticoagulants. *Thromb Haemost*. 1997; 77:690–6. [PubMed: 9134644]
- [40]. Kelton JG, Warkentin TE. Heparin-induced thrombocytopenia: a historical perspective. *Blood*. 2008; 112:2607–16. [PubMed: 18809774]
- [41]. Martel N, Lee J, Wells PS. Risk for heparin-induced thrombocytopenia with unfractionated and low-molecular-weight heparin thromboprophylaxis: a meta-analysis. *Blood*. 2005; 106:2710–5. [PubMed: 15985543]
- [42]. Wang S, Zhang Y, Wang H, Dong Z. Preparation, characterization and biocompatibility of electrospinning heparin-modified silk fibroin nanofibers. *Int J Biol Macromol*. 2011; 48:345–53. [PubMed: 21182858]
- [43]. Zhao W, McCallum SA, Xiao Z, Zhang F, Linhardt RJ. Binding affinities of vascular endothelial growth factor (VEGF) for heparin-derived oligosaccharides. *Biosci Rep*. 2012; 32:71–81. [PubMed: 21658003]
- [44]. Norrby K. Low-molecular-weight heparins and angiogenesis. *APMIS*. 2006; 114:79–102. [PubMed: 16519745]
- [45]. Norrby K, Nordenhem A. Dalteparin, a low-molecular-weight heparin, promotes angiogenesis mediated by heparin-binding VEGF-A in vivo. *APMIS*. 2010; 118:949–57. [PubMed: 21091776]
- [46]. Norrby K, Ostergaard P. A 5.0-kD heparin fraction systemically suppresses VEGF165-mediated angiogenesis. *Int J Microcirc Clin Exp*. 1997; 17:314–21. [PubMed: 9527522]
- [47]. Mousa SA, Mohamed S. Inhibition of endothelial cell tube formation by the low molecular weight heparin, tinzaparin, is mediated by tissue factor pathway inhibitor. *Thromb Haemost*. 2004; 92:627–33. [PubMed: 15351861]
- [48]. Saitow C, Kaplan DL, Castellot JJ Jr. Heparin stimulates elastogenesis: application to silk-based vascular grafts. *Matrix Biol*. 2011; 30:346–55. [PubMed: 21600981]

- [49]. Perkins SJ, Nan R, Li K, Khan S, Miller A. Complement factor H-ligand interactions: self-association, multivalency and dissociation constants. *Immunobiology*. 2012; 217:281–97. [PubMed: 22137027]
- [50]. Gorbet MB, Sefton MV. Biomaterial-associated thrombosis: roles of coagulation factors, complement, platelets and leukocytes. *Biomaterials*. 2004; 25:5681–703. [PubMed: 15147815]
- [51]. Rauterberg EW, Ritz E. Bioincompatibility of dialysis membranes: factor H binding correlates inversely with complement activation indicating a local imbalance of involved proteases/anti-proteases. *Adv Exp Med Biol*. 1988; 240:365–75. [PubMed: 2977522]
- [52]. Andersson J, Larsson R, Richter R, Ekdahl KN, Nilsson B. Binding of a model regulator of complement activation (RCA) to a biomaterial surface: surface-bound factor H inhibits complement activation. *Biomaterials*. 2001; 22:2435–43. [PubMed: 11511041]
- [53]. Khan S, Nan R, Gor J, Mulloy B, Perkins SJ. Bivalent and co-operative binding of complement factor H to heparan sulfate and heparin. *Biochem J*. 2012; 444:417–28. [PubMed: 22471560]

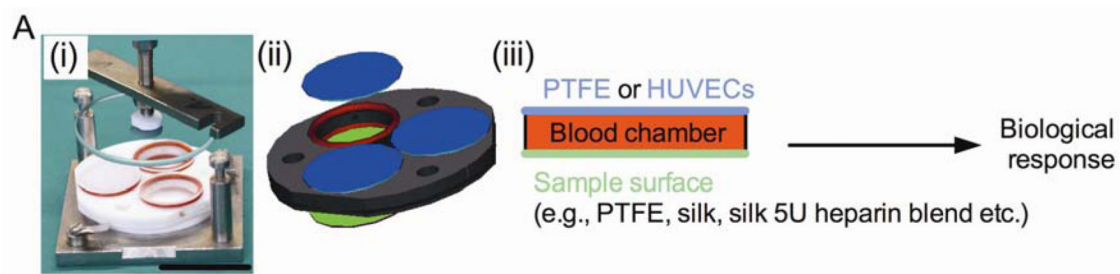


Figure 1.

Experimental design of the study: (i) photograph and (ii) diagram of incubation chamber, (iii) sample arrangement in chamber.

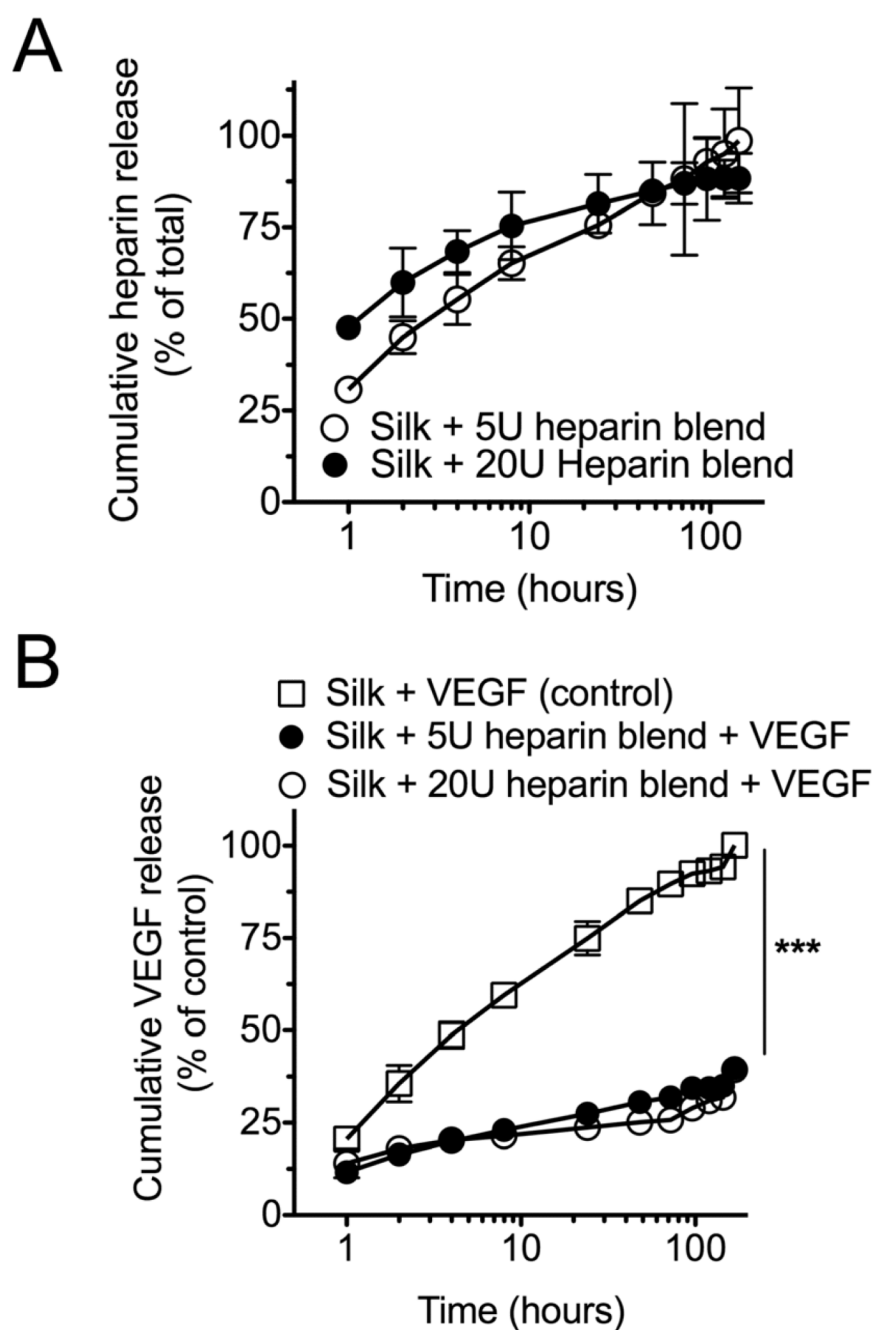


Figure 2.

Heparin and VEGF release from silk substrates. **(A)** Heparin release from silk heparin blends containing 5U or 20U. **(B)** Cumulative VEGF release from pure silk films (Silk + VEGF) or substrates that contained 5U or 20U of admixed heparin (Silk + 5U heparin blend + VEGF or Silk + 20U heparin blend + VEGF). (Statistical differences between the control and treatment groups were determined using one-way ANOVA and Bonferroni *post hoc* test *** $P < 0.001$; \pm SD; $n = 3$).

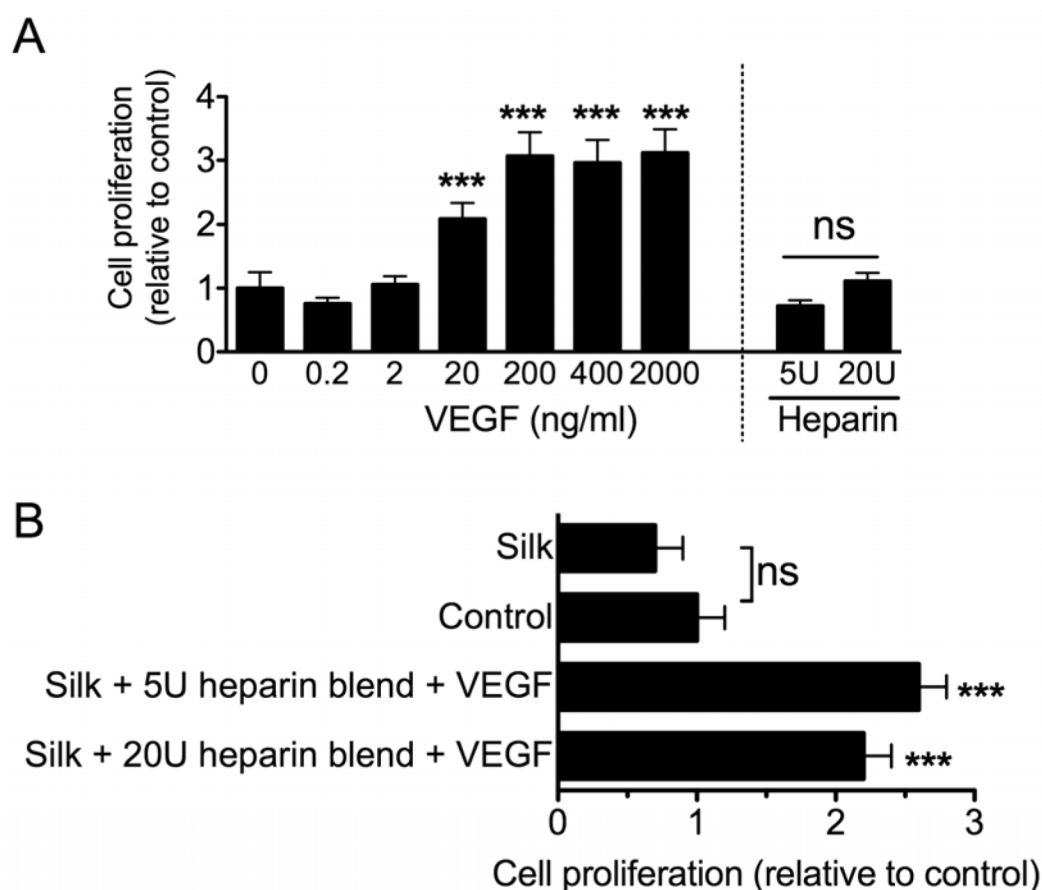


Figure 3.

Biological response of endothelial cells towards VEGF loaded silk substrates. **(A)** Endothelial proliferation following a 3 day exposure to diffusible VEGF or heparin. **(B)** Cellular response towards VEGF loaded silk substrates. The control group refers to the baseline in the absence of any treatment. Samples were pure silk films (Silk + VEGF) or substrates that contained 5U or 20U of admixed heparin (Silk + 5U heparin blend + VEGF or Silk + 20U heparin blend + VEGF). (Statistical differences between the control and treatment groups were determined using one-way ANOVA and Dunnett's multiple comparison *post hoc* test * $P < 0.05$; ** $P < 0.01$ *** $P < 0.001$; \pm SD; $n=3$).

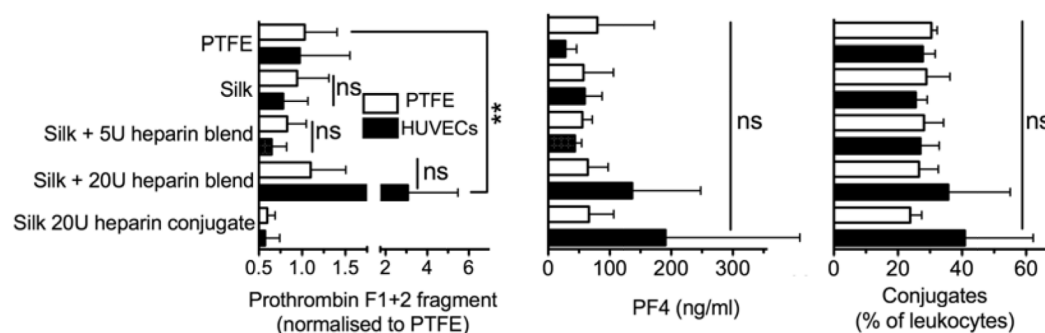


Figure 4.

Hemostasis response of whole human blood to silk substrates. All samples were incubated for 2 h with blood in the presence or absence of endothelial cells and the hemostasis response was measured. Plasma levels of prothrombin F1+2 fragment, platelet factor 4 (PF4) and leukocyte conjugates served as indicators for hemostasis. Studies were conducted with polytetrafluoroethylene (PTFE), pure silk films (Silk), silk films that contained 20U of conjugated heparin (Silk 20U heparin conjugate), silk heparin blended films that contained 5U (Silk + 5U heparin blend) or 20U of heparin (Silk + 20U heparin blend). Dashed line for the conjugates indicates levels following lipopolysaccharide stimulation. (Statistical differences between sample pairs examining the impact of endothelial cells were analyzed with the Student's *t*-test whereas differences between the PTFE control and silk films were determined using one-way ANOVA and Dunnett's multiple comparison *post hoc* test * $P < 0.05$; ** $P < 0.01$; \pm SD; $n = 3$).

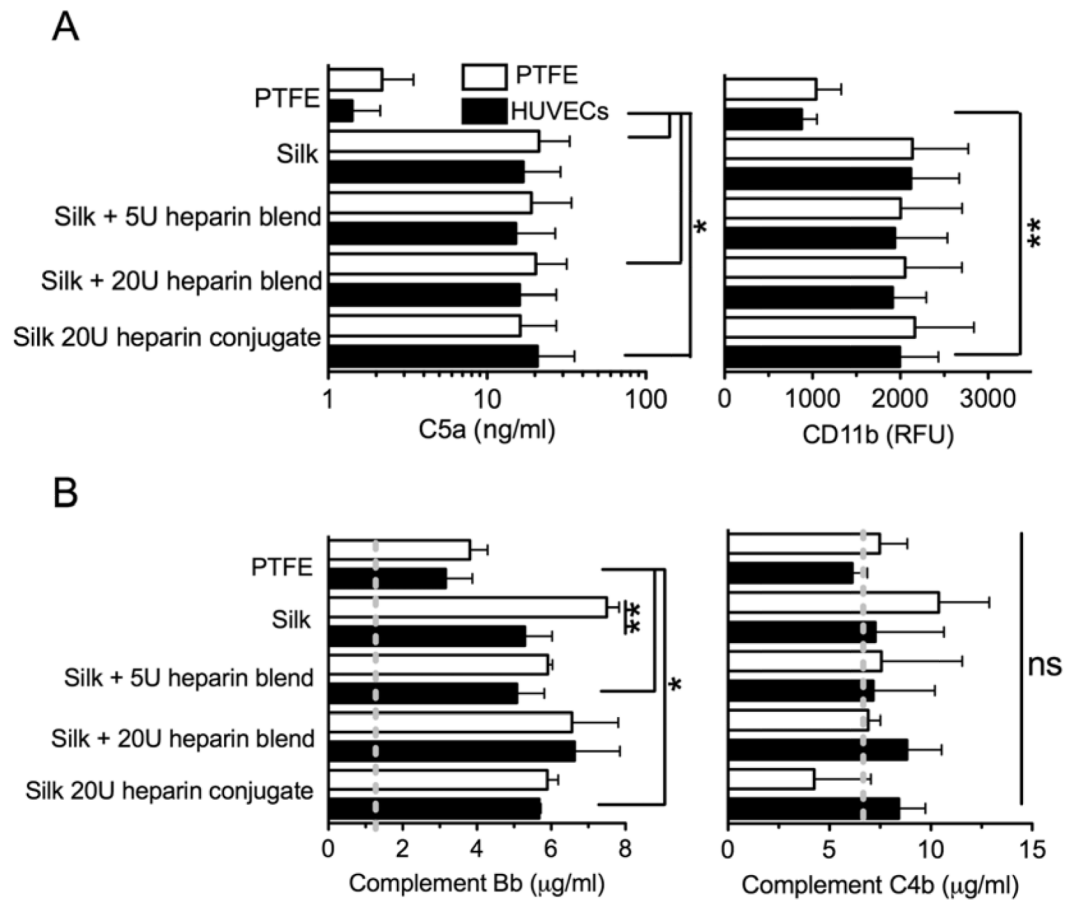


Figure 5.

Inflammatory response of whole human blood to silk substrates. All samples were incubated with blood for 2 h and inflammatory response was measured. **(A)** Complement fragment C5a in the plasma and leukocyte activation by monitoring CD11b expression. **(B)** Complement levels of Bb and C4d in the plasma as an indicator for the alternate and classical pathway, respectively. Dashed lines indicate initial levels. (Statistical differences between sample pairs examining the impact of endothelial cells were analyzed with the Student's t-test, whereas differences between PTFE control and silk films were determined using one-way ANOVA and Dunnett's multiple comparison *post hoc* test $*P<0.05$; $**P<0.01$; \pm SD; $n=3$). Samples are defined in Figure 4 and the experimental set up is shown in Figure 1.

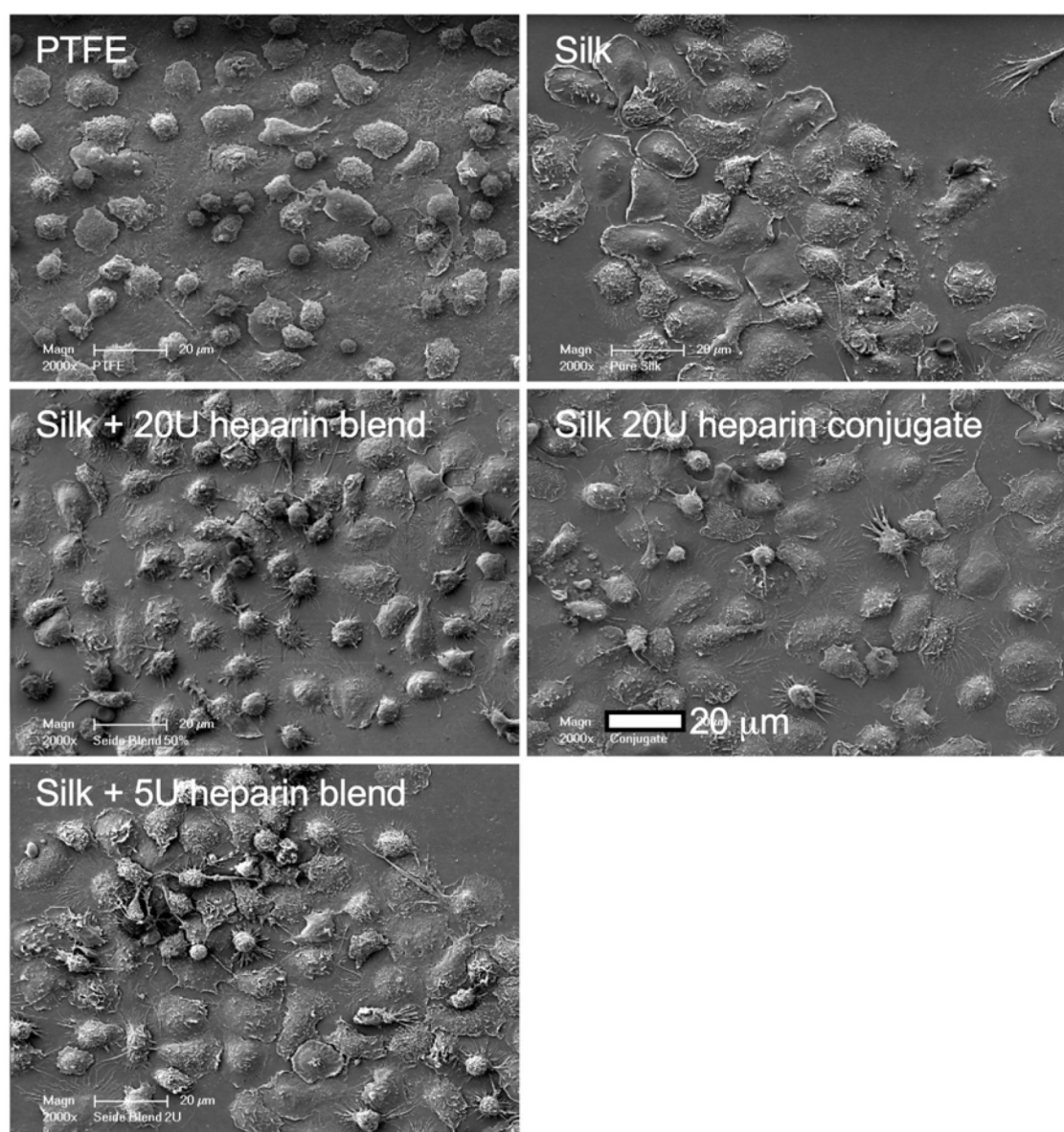


Figure 6. Qualitative assessment of silk substrates exposed to whole human blood. Representative scanning electron micrographs of samples following a 2 h blood incubation. Images derived from PTFE co-incubation studies; comparable results were obtained for endothelial cell co-incubation studies. Samples are defined in Figure 4.

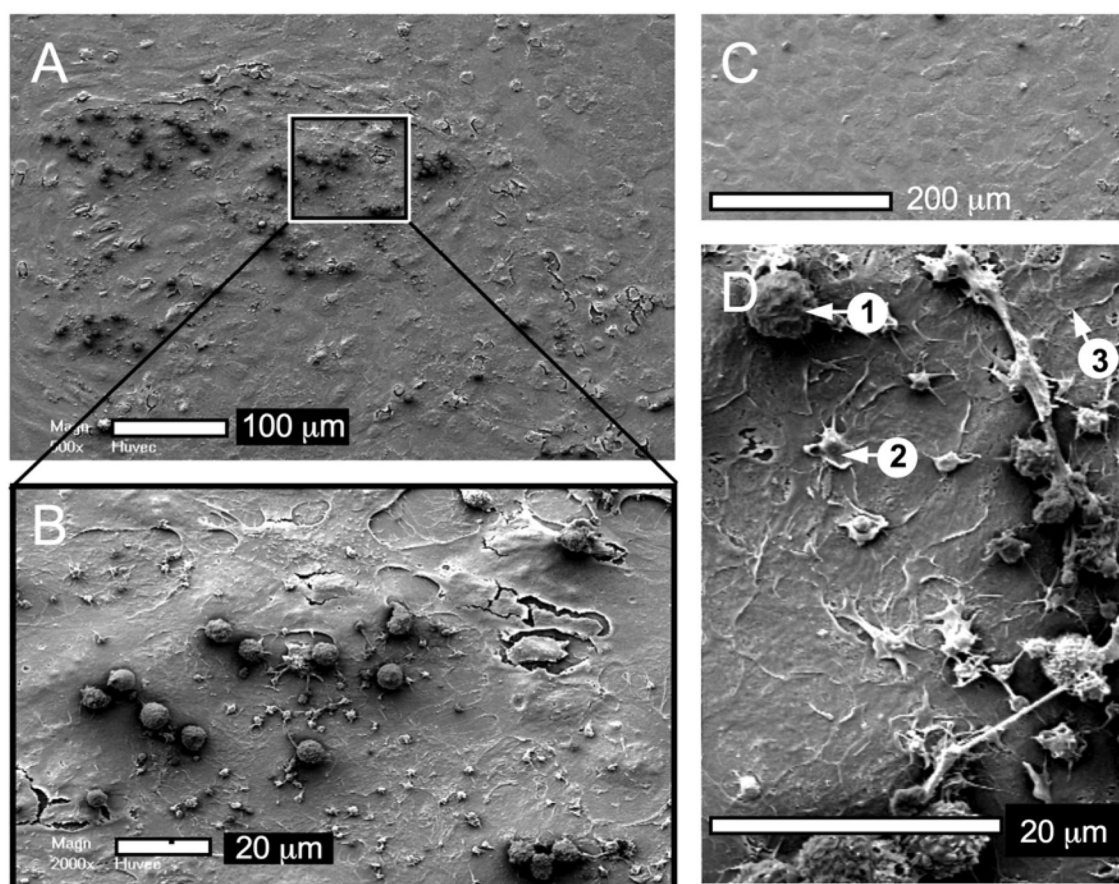


Figure 7.

Quantitative assessment of surface-associated leukocytes following a 2 h whole human blood incubation. Scanning electron micrographs are from the PTFE co-incubation experiments but similar results were obtained with the other sample groups. **(A)** Low magnification of endothelial monolayer with a zoomed area **(B)** showing attached leukocytes, platelets, and endothelial cells (cracks are artifacts introduced during sample preparation). **(C)** Confluency of endothelial monolayer, **(D)** examples of adherent (1) leukocytes, (2) platelets with pseudopods and (3) endothelial cells; granulocytes are absent.